NASA TECHNICAL MEMORANDUM

NASA TMX-64655

LOW-g ACCELEROMETER TESTING

By Bobby F. Walls
Astrionics Laboratory

Miller S. Vaughan
Sperry Rand Corporation

January 13, 1972

NASA

George C. Marshall Space Flight Center
Marshall Space Flight Center, Alabama

MSFC - Form 3190 (Rev June 1971)

TECHNICAL REPORT STANDARD TITLE PAGE

1. REPORT NO.	2. GOVERNMENT ACCESSION NO.	3. RECIPIENT'S CATALOG NO.
NASA TM X- 64655		

4. TITLE AND SUBTITLE	5. REPORT DATE
Low-g Accelerometer Testing	January 13, 1972
	6. PERFORMING ORGANIZATION CODE

7. AUTHOR(S)	8. PERFORMING ORGANIZATION REPORT #
Bobby F. Walls and Miller S. Vaughan	

9. PERFORMING ORGANIZATION NAME AND ADDRESS	10. WORK UNIT NO.
George C. Marshall Space Flight Center Marshall Space Flight Center, Alabama 35812	11. CONTRACT OR GRANT NO.
	13. TYPE OF REPORT & PERIOD COVERED
12. SPONSORING AGENCY NAME AND ADDRESS	Technical Memorandum
National Aeronautics and Space Administration Washington, D. C. 20546	14. SPONSORING AGENCY CODE

15. SUPPLEMENTARY NOTES

Prepared by Astrionics Laboratory, Science and Engineering

16. ABSTRACT

This report covers eight different types of low-g accelerometer tests on the Bell miniature electrostatically suspended accelerometer (MESA) which is known to be sensitive to less than 10^{-7} earth's gravity. These tests include a mass attracting scheme, Leitz dividing head, Wild theodolite, precision gage blocks, precision tiltmeters, Hilger Watts autocollimator, Razdow Mark II autocollimator, and laser interferometer measuring system. Each test is described and a comparison of the results is presented.

The output of the MESA was as linear and consistent as any of the available devices were capable of measuring. Although the extent of agreement varied with the test equipment used, it can only be concluded that the indicated errors were attributable to the test equipment coupled with the environmental conditions.

17. KEY WORDS	18. DISTRIBUTION STATEMENT
Accelerometer Low-g tests Mass attraction Gravity	Unclassified - Unlimited Bobby F. Walls

19. SECURITY CLASSIF. (of this report)	20. SECURITY CLASSIF. (of this page)	21. NO. OF PAGES	22. PRICE
Unclassified	Unclassified	47	$3.00

MSFC - Form 3292 (May 1969)

TABLE OF CONTENTS

TABLE OF CONTENTS (Concluded)

LIST OF ILLUSTRATIONS

LIST OF ILLUSTRATIONS (Concluded)

TECHNICAL MEMORANDUM X-64655

LOW-g ACCELEROMETER TESTING

INTRODUCTION

Description

The Bell miniature electrostatically suspended accelerometer (MESA) has rebalancing pulses which are periodically counted and thus used to determine the forces acting on the proof mass. The pulse counts therefore represent a series of definite integrations of the input forces.

The sensitivity of the MESA, which is known to be less than 10^{-7} g, is beyond the measuring capability of any of the available precision measuring devices that have a range great enough to cover that of the MESA.

The low-g range of the MESA is about 500 microgravities (μg) from the zero point or 1000 μg full range; 500 μg is the equivalent of a total tilt angle of 103 arc-sec in a 1-g field. The high-g range is about 10 times the low-g range.

Other Tests

Previous tests have been made on the MESA with limited success. A space flight evaluation was made by Daniel J. Lesco at Lewis Research Center [1]. Accelerations in the order of 60 μg were measured from flight data.

The sensitivity of the MESA was measured in a mass attraction test; a response to 10^{-7} earth's gravity was shown to exist. According to Reference 2, the MESA can be calibrated by this means. The calibration uses a computerized filtering technique on the data to separate the mass attraction effects from the interference effects. A description of the test and a plot of the test data are presented in this report.

Present Tests

To evaluate the precision and linearity of the MESA in a 1-g field and to determine the most precise method of test, several arrangements and types of precision equipment were used. The environmental problems in this testing are also described to the extent that they could be analyzed.

For comparison purposes, the scale factor linearity was tested over at least 80 percent of the MESA range in the low-g range with the various test setups. A few tests were also made in the high-g range.

TEST EQUIPMENT

Location

These tests were run in a test area with a granite pedestal on an isolated foundation at the Astrionics Laboratory. This facility provided the most suitable test stand available in the area but was somewhat short of the near perfect environment required for measuring the very small forces involved.

Equipment Used

In addition to the MESA electronics package, the following equipment was used:

1. Monitor panel, Bell Aerospace Co., Marshall Electronic Test Set.
2. Voltmeter, Hewlett Packard Model 2401A (used as a pulse counter).
3. Dual channel strip chart recorder, Mosley Model 1100B.
4. Power Supplies, Electronic Measurements Model PRO 125.1 (two units used).
5. Printer/digital to analog converter, Hewlett Packard Model 562A.
6. Tiltmeter, Ideal Aerosmith Model DCTM31.

7. Block and tackle, 272 kg (3-ton), 3 to 1 leverage.

8. Electric hoist, 453 kg (1/2-ton).

9. Square steel hoisting basket: height, 101.6 cm (40 in.); width and depth, 64.77 cm (25.5 in.); capable of lifting at least 272 kg (3 tons).

10. Angle iron braces, 3.81 × 3.81 × 0.635 cm (1.5 × 1.5 × 0.75 in.) (as many as necessary used).

11. Lead cubes, 10.16 cm (4 in.) side (100 used).

12. Lead cubes, 5.08 cm (2 in.) side (100 used).

13. Wood cubes, 10.16 cm (4 in.) side (50 used).

14. Wood cubes, 5.08 cm (2 in.) side (50 used).

The following equipment was used as primary testing systems:

1. Items 11 and 12 above.

2. Precision dividing head, Leitz.

3. Theodolite, Wild (as an autocollimator).

4. Precision gage blocks, Pratt Whitney.

5. Laser interferometer measuring system, General Dynamics NASA Contract No. NAS8-20568.

6. Dual axis autocollimator, Hilger Watts Model TA-51.

7. Automatic autocollimator, Razdow Model Mark II.

Interconnections

Figure 1 shows the basic interconnections for the MESA and the tiltmeter. The MESA fixtures and the tiltmeter were mounted on the same granite pedestal and were used in all of the tests except those run with the Leitz dividing head and the Wild theodolite. In these two tests, the tiltmeter was not being monitored.

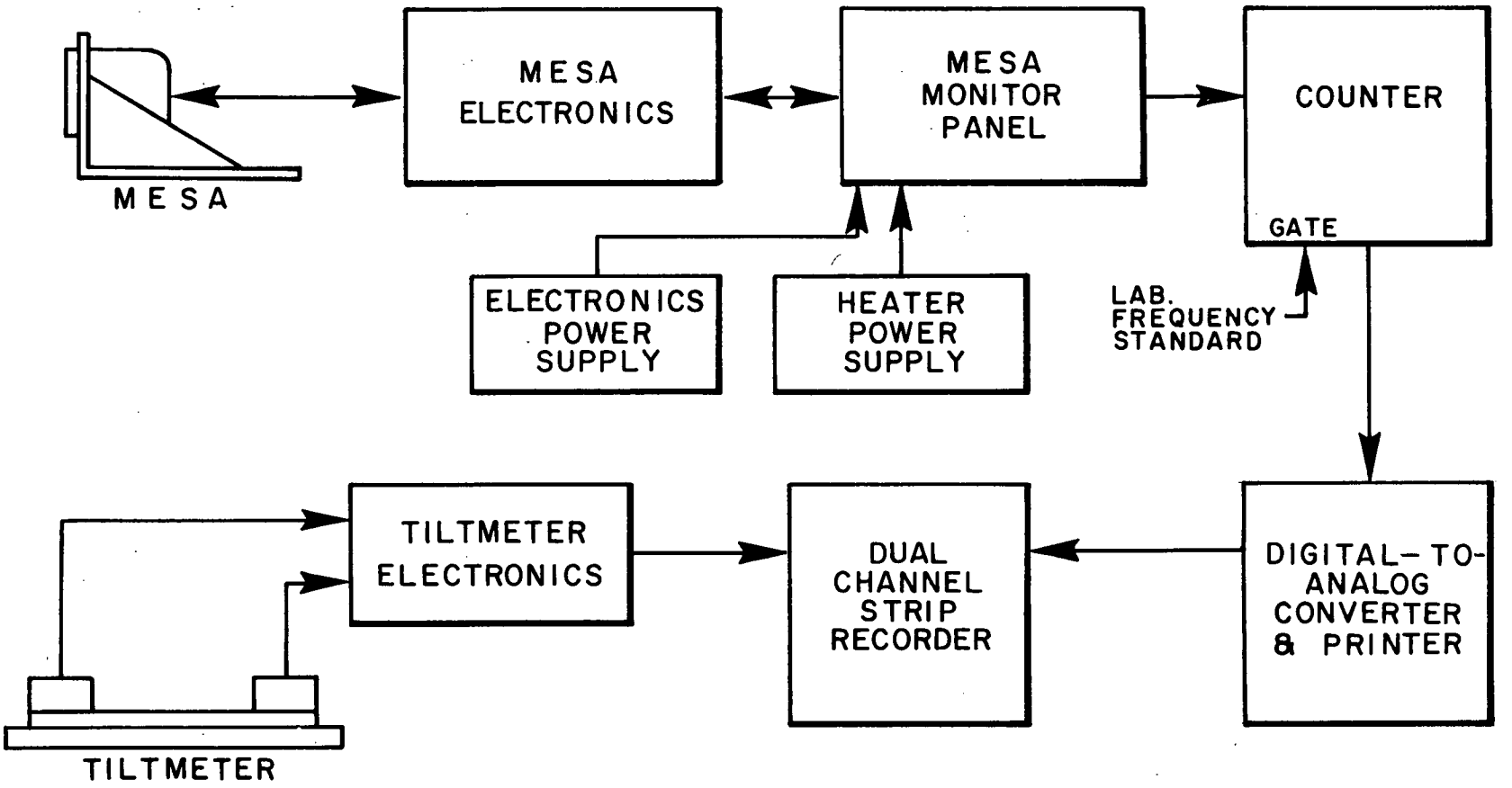

Figure 1. Interconnections for Bell MESA and Ideal Aerosmith tiltmeter.

PROBLEMS IN TESTING

The main limitations in the precision with which the MESA can be tested are caused by (1) temperature variations in the test equipment and fixtures, (2) local seismic variations, (3) self-contained interference in the MESA, and (4) limitations of the test equipment.

Heat Interferences

Several watts of heat are given off by the ovens in the MESA and the electronic package. The thermal gradients introduced into the holding fixture by this dissipation cause the fixture to distort and reposition the MESA when a change occurs in (1) the ambient temperature, (2) the movement of the air around the fixture, or (3) the induced temperature by radiation.

A few experimental tests were run which indicated that the fixture position deformed enough to change as much as 3 arc-sec for each degree (centigrade) of change in the temperature of the fixture. However, this varied with each test.

The following steps were taken to minimize the temperature effect on the test data:

1. Plexiglass hoods were placed over the accelerometer, tilting fixture, and electronic package.

2. The data used in this report were taken during the more stable temperature periods in the test area since no adequate method of controlling or compensating for temperature change with the necessary precision was available.

3. Minimum integration time (usually 100-s) was used to minimize the effect from general changes in temperature which would eventually change the temperature under the hood. However, this was a trade-off with the need for greater periods to integrate the higher frequencies of the seismic variations.

For the mass attraction tests, double hoods were used. One hood was placed over the accelerometer and the holding fixture. The second hood was placed over the first and also over the electronic package. The inside hood and parts of the outside hood were covered with aluminum foil.

The aluminum foil for radiation shielding was found to be necessary after the first trial run in which the data indicated that the accelerometer was reacting in the wrong direction at several times the expected magnitude.

Preliminary tests with sheets of cardboard indicated that the MESA was probably sensing changes in the position of the fixture. The movement of the mass basket up and down apparently produced a change in reflected radiation from the mass to the fixture which produced movement from temperature distortion. The setup was allowed to stabilize for at least 24 hr and until the outputs of the MESA and tiltmeter indicated maximum stabilization.

Seismic Interferences

The seismic variations were less of a problem than the temperature. They could usually be traced to their source (earthquakes, tides, building vibration, noises, etc.) and in some cases could be avoided by scheduling for quiet periods.

Vibrations with frequencies of greater than 1 Hz could be detected on the DCTM31 tiltmeter when used with a high-gain recorder. The actual amplitude could not be determined because of the dampening of the tiltmeter in this range. These were probably caused by the air conditioning system, etc. This interference was mostly integrated by the MESA when using 100-s sampling periods.

A random variation could be observed on the DCTM31 tiltmeter which started and stopped with the normal working hours at the laboratory. This variation normally has a period of from less than 1 s up to 1 hr. The amplitude was seldom over 0.1 arc-sec but was recorded by both the MESA and the tiltmeter recorders and could therefore be accounted for in the comparison tests. This was avoided in the mass attraction test by running the test in the normal off-work hours.

Another seismic variation occasionally present with a greater period and amplitude appeared to have been caused by local rain accumulations and run off. This variation had a period from one to several days and an amplitude of as high as 5 arc-sec. This also was recorded by both the tiltmeter and the MESA. Tests were not normally run during these variations because they were also accompanied by unstable temperature conditions.

Earth tremors were also recorded on both the tiltmeter and the MESA but because of their infrequent nature and characteristic waveform, they were easily identified. The times and amplitudes of the occurrences were correlated with the U. S. Coast and Geodetic Survey reports. If necessary, tests were delayed until the tremors had run their course.

Self-Contained Interference

The self-contained interference in the MESA could not be determined because minor temperature and seismic variations were always present. However, no detectable variation could be attributed to the heater's cycling or normal power supply variations.

In the low-g mode, a maximum of about 0.4 μg variation was present when using a 10-s sample period. With a 100-s sample period, this was reduced to about 0.1 μg. These variations were several magnitudes larger when the hoods were not used; they were also independent of the magnitude of the input.

Test Equipment Limitations

The only available direct reading systems that have comparable sensitivities with the MESA are the Ideal Aerosmith tiltmeters, Models DCTM31 and DCTM11. The DCTM31 has a range of only 1.53 μg and the DCM11 has a range of about 12 μg in their most sensitive modes. The DCTM31 was used to record the seismic variations to which the test stand was subjected during the tests.

The laser interferometer system had a limited range but it was ample for the low-g range of the MESA. The other systems had ample ranges for the MESA in either the high- or low-g modes but some were found to lack the expected correlation.

MASS ATTRACTION TEST

Test Description

Figure 2 shows the test setup for the mass attraction test. The lead mass was raised and lowered to provide a change of distance and angle between the mass and the input of the MESA.

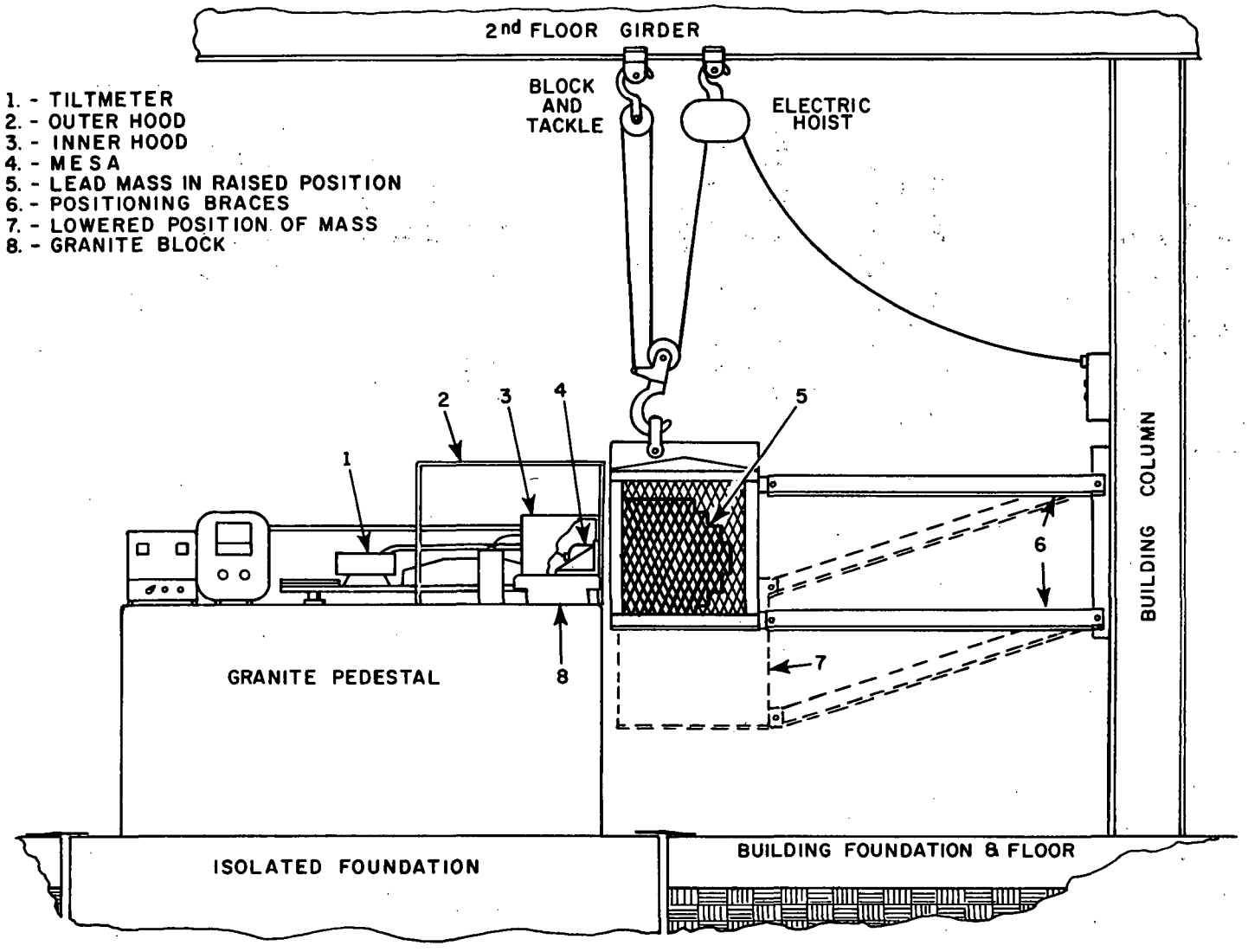

Figure 2. Mass attraction text setup.

Hoisting the mass from the overhead girders provided a minimum of position transfer to the isolated foundation from the building structure. The positioning braces which were hinged to the building column caused less than 2.54 cm (1 in.) of lateral movement to the mass. With the arrangement shown, this could have caused the MESA to react in opposition to the gravitational force of the mass had there been motion transfer through the structure.

Mass Description

The mass consisted of one hundred 5.08-cm (2-in.) and one hundred 10.16-cm (4-in.) cubes of lead arranged in a steel basket in the approximate form of a sphere with an extended and flattened end. The flattened end faced the MESA and was moved as closely as possible to the MESA in the position of maximum effect. The voids in the basket were filled with wooden blocks.

Method of Calculation

A change of 23 nanogravities was achieved when the mass was moved from one to the other of the selected positions.

The following method was used to calculate the gravitational attraction of the mass on the MESA.

From the general equation

$$F = \gamma \frac{Mm}{d^2} ,$$

the force or acceleration on the proof mass is

$$F = \frac{Mm \cos \theta}{d^2}$$

or

$$A = \frac{M \cos \theta}{d^2}$$

where

M = mass of an attracting body.

m = proof mass of the MESA.

F = force of attraction.

γ = universal gravity constant.

d = straight line distance between the CG of the masses.

θ = angle between the sensitive axis of the MESA and d.

A = acceleration acting on the MESA because of the attracting force.

By considering the proof mass of the MESA as a point mass and the attracting mass as a group of 5.08-cm (2-in.) cubes with point masses of their centers, the total attraction is the sum of the forces exerted by these point masses on the proof mass.

An orthogonal coordinate system XYZ was used as shown in Figure 3 to determine the effect of each 5.08-cm (2-in.) cube on the proof mass by applying the equation

$$A = \frac{\gamma M' X}{X^2 + Y^2 + Z^2} \quad 3/2 .$$

The total attraction consisted of the sum of the attractions of nine hundred 5.08-cm (2-in.) cubes having the positions of greatest affect on the proof mass (total mass 1858.8 kg).

Test Results

Figure 4 shows the direct results of a successful run of the mass attraction test. The mass was raised and lowered 25 times as shown by the O's and X's on the plot. The vertical scale is extended to show the mass attraction effects through the relatively large general change caused by a

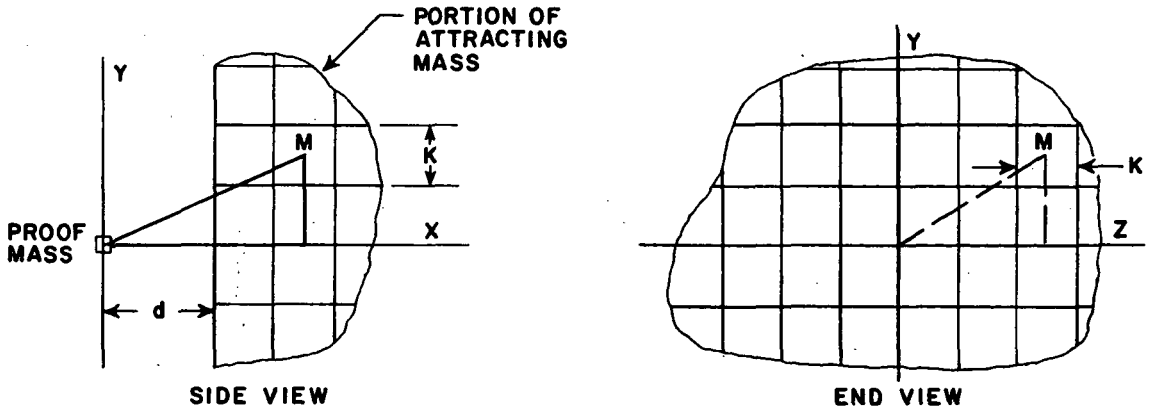

SAMPLE COORDINATES $(d + \frac{3}{2}K), (\frac{3}{2}K), (\frac{5}{2}K)$

K = 5.08 cm (2 in.)

M = 206.45 grams

Figure 3. Mass point location.

small and gradual change in temperature in the test area. The normal fluctuations in the MESA account for the inconsistencies in the cycles of the mass movement effects. The horizontal or test sequence scale covers a period of 8 min/cycle. The mass was held in the upper intermediate (not shown)[1] and the low positions for a sampling period of 100-s. Also included and not shown are the times (20-s each) to move the mass, i.e., a total of 120 s or 2 min for each reading.

COMPARISON TESTS

General

For the comparison test, the procedure for linearity and scale factor was similar. The size of the test increments was varied to suit the testing equipment. In general, the following procedure was used:

1. The MESA was turned on with specified voltages and adjusted to a near zero position, i.e., input horizontal.

1. The intermediate positions were necessary for the calibration technique in Reference 2 but not for this display.

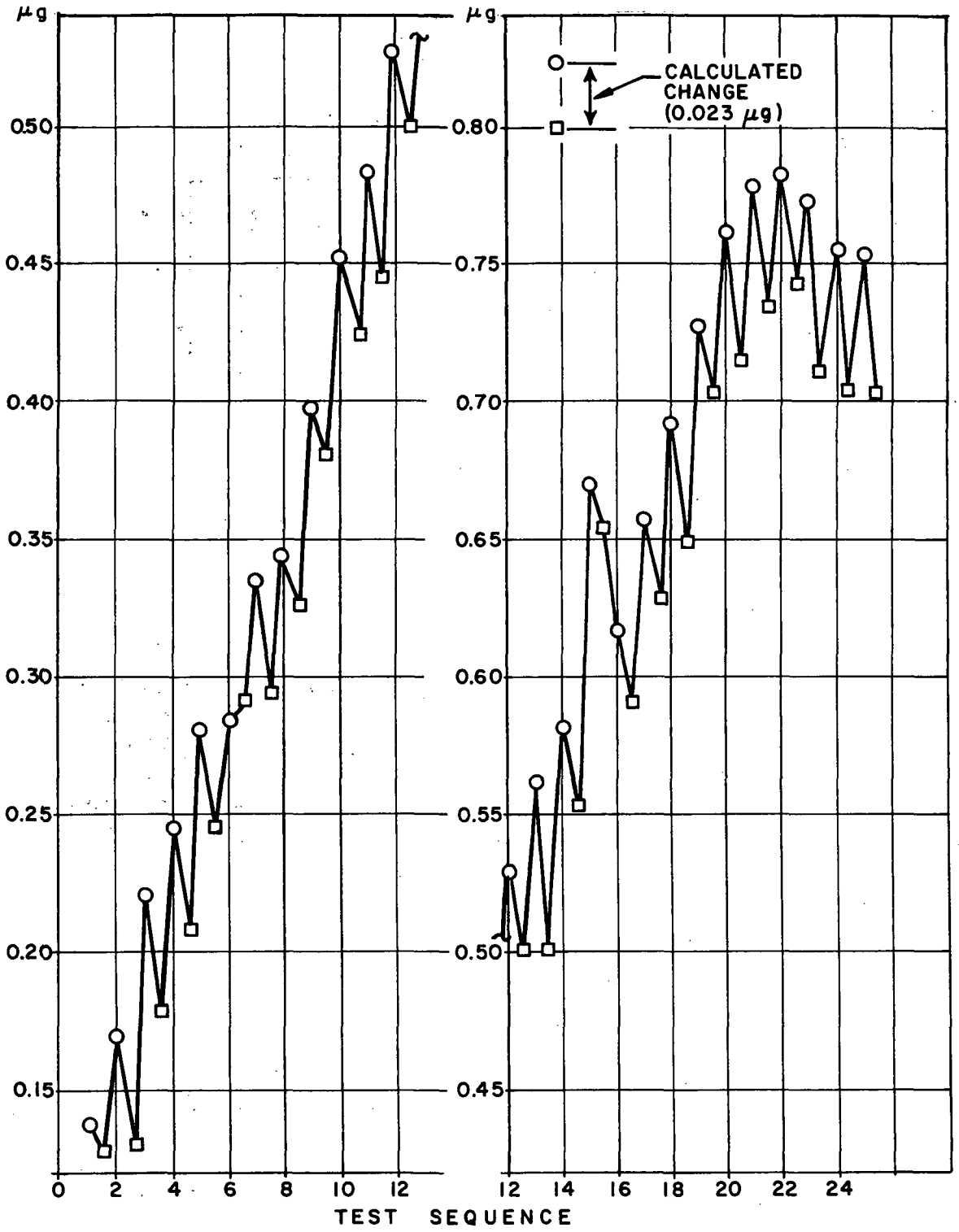

Figure 4. Mass attraction test data.

2. The systems were allowed to reach maximum stability as indicated on a strip chart. This generally required 24 hr with the hood over the MESA. (The tiltmeter system was left on continuously.)

3. The MESA was then adjusted to the starting position and the first readings were taken after a short period of stabilization.

4. The MESA was then moved to the next position and the next readings were taken after stabilization.

5. Step 4 was repeated until the MESA had been moved through the major part of its range, usually including return to the starting position.

To make graphical comparisons from several types of tests, the results of one or more runs of each of the tests were plotted in a similar manner. The vertical is scaled in μg error and horizontal in μg range of the MESA. Each plotted line represents a sample of comparison data between two test points of the MESA with the primary testing device. The length and the horizontal position of the plotted line indicate the size and position of the sample in the MESA range. The vertical position of the plot indicates the error in μg between the MESA (using an average scale factor) and the primary testing device.

The average scale factor of the MESA was calculated from the extreme ends of the range for which data were taken in that test. The necessary calculations to convert the output of the primary testing device to μg are shown for each device used. When necessary, tiltmeter readings were used to correct the input values for small seismic variations.

The number associated with each plot shows the sequence in the data in which that plot was taken. This was done so that any nonrandom variation in the progress of the test could be observed since it may indicate nonlinearity of either the test equipment or the MESA or a problem in the test arrangement.

Leitz Dividing Head

Figures 5 and 6 are error plots of the scale factor data taken in the acceptance tests of the MESA at the Astrionics Laboratory, MSFC (solid plots) and the test data provided with the MESA from Bell Aerospace Corp. (dotted plots). The MESA is run in the low-g mode in Figure 5 and in the high-g mode in Figure 6.

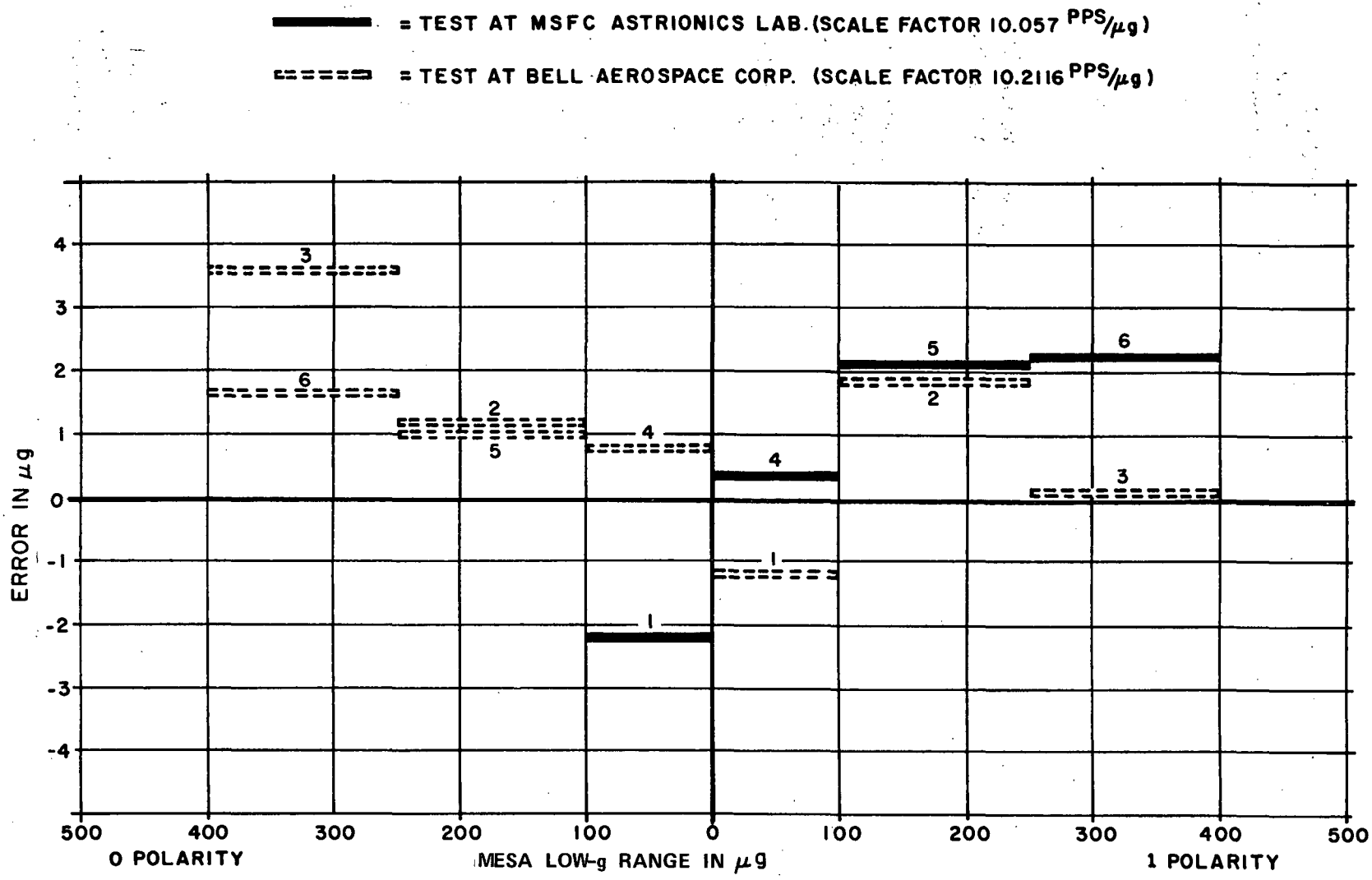

Figure 5. MESA and Leitz dividing head (low g).

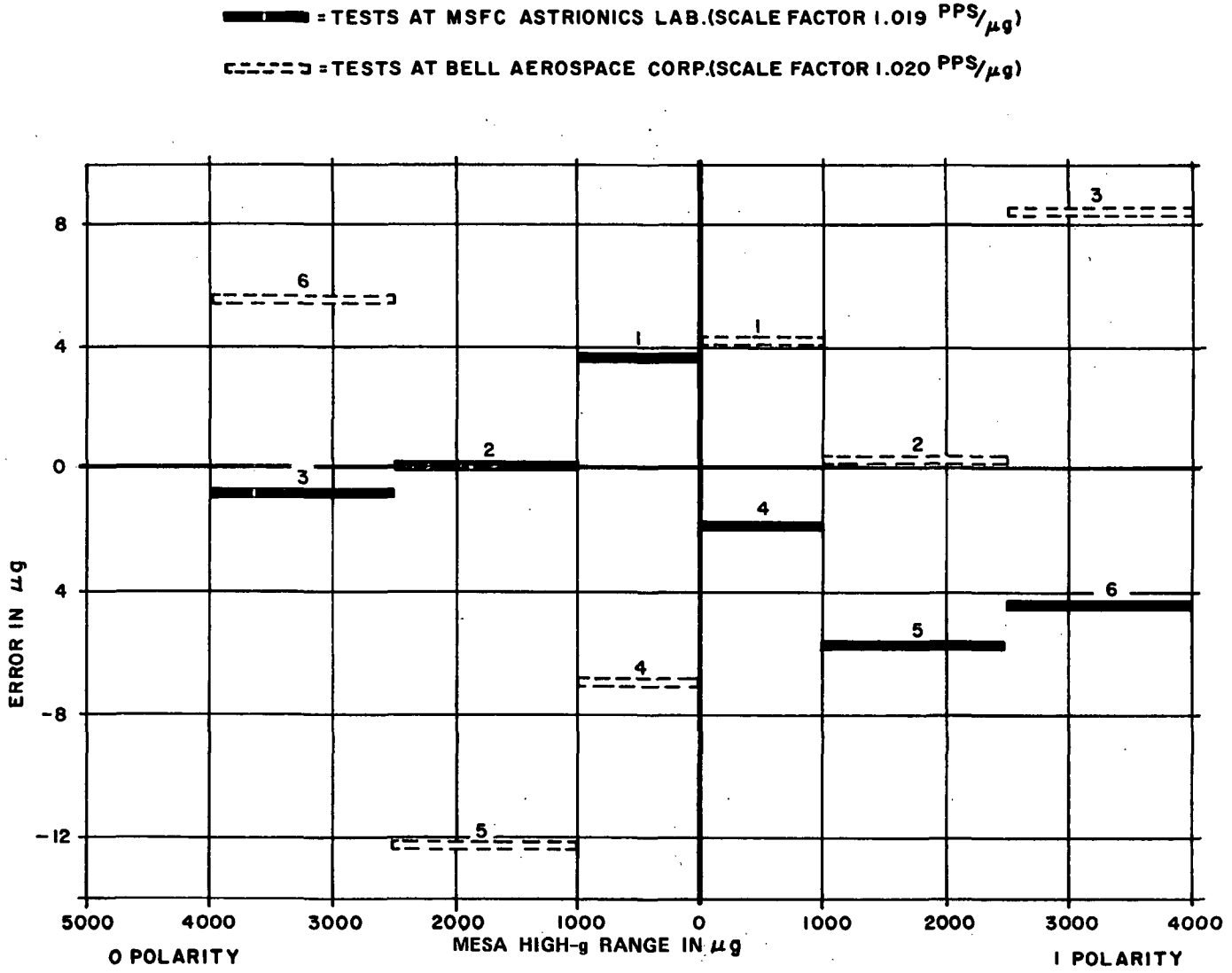

Figure 6. MESA and Leitz dividing head (high g)

In these tests (solid plots), the MESA was bolted to a right-angle, stainless-steel fixture which was in turn bolted to the surface plate of the dividing head. With the dividing head axis in the horizontal position, the main vernier scale was used to determine the tilt angle.

The resolution of the dividing head is 2 arc-sec. The maximum overall error is less than 4 arc-sec. Since 2 arc-sec is equivalent to about 9.7 μg, the results of the tests in Figures 5 and 6 are about as close as can be expected on the basis of the testing device limitations alone. The undisturbed variations on the MESA are included in the variation of the plot errors.

For the very small angles in these tests, the angle from the horizontal in μ rad is equivalent to the MESA input in μg.

Wild Theodolite

Figures 7 and 8 are plots of low-g and high-g ranges of the MESA using the Wild theodolite as an autocollimator for the prime measuring device. The theodolite was mounted on a steel standard adjacent to the dividing head test stand and focused on a mirror clamped to the MESA holding fixture.

Although the theodolite has a considerably more accurate scale than that of the dividing head, a comparison of the test results of Figures 5 and 6 with Figures 7 and 8 shows a degradation in the test by virture of the greater error spread of the test samples. This was probably caused by the test stand arrangement which was more vulnerable to environmental conditions. The theodolite may also have been slightly displaced when adjustments were made.

Gage Blocks

Figure 9 shows an arrangement in which precision gage blocks were used for the primary test device. The span or lever arm of the test fixture was 25.4 cm (10 in.). The gage blocks were used in pairs as shown at the top of Figures 10 and 11.

By removing one block and inserting the other, a small angular change was applied to the fixture. The affected area in the range of the MESA was determined by adjusting the feet under the granite surface block.

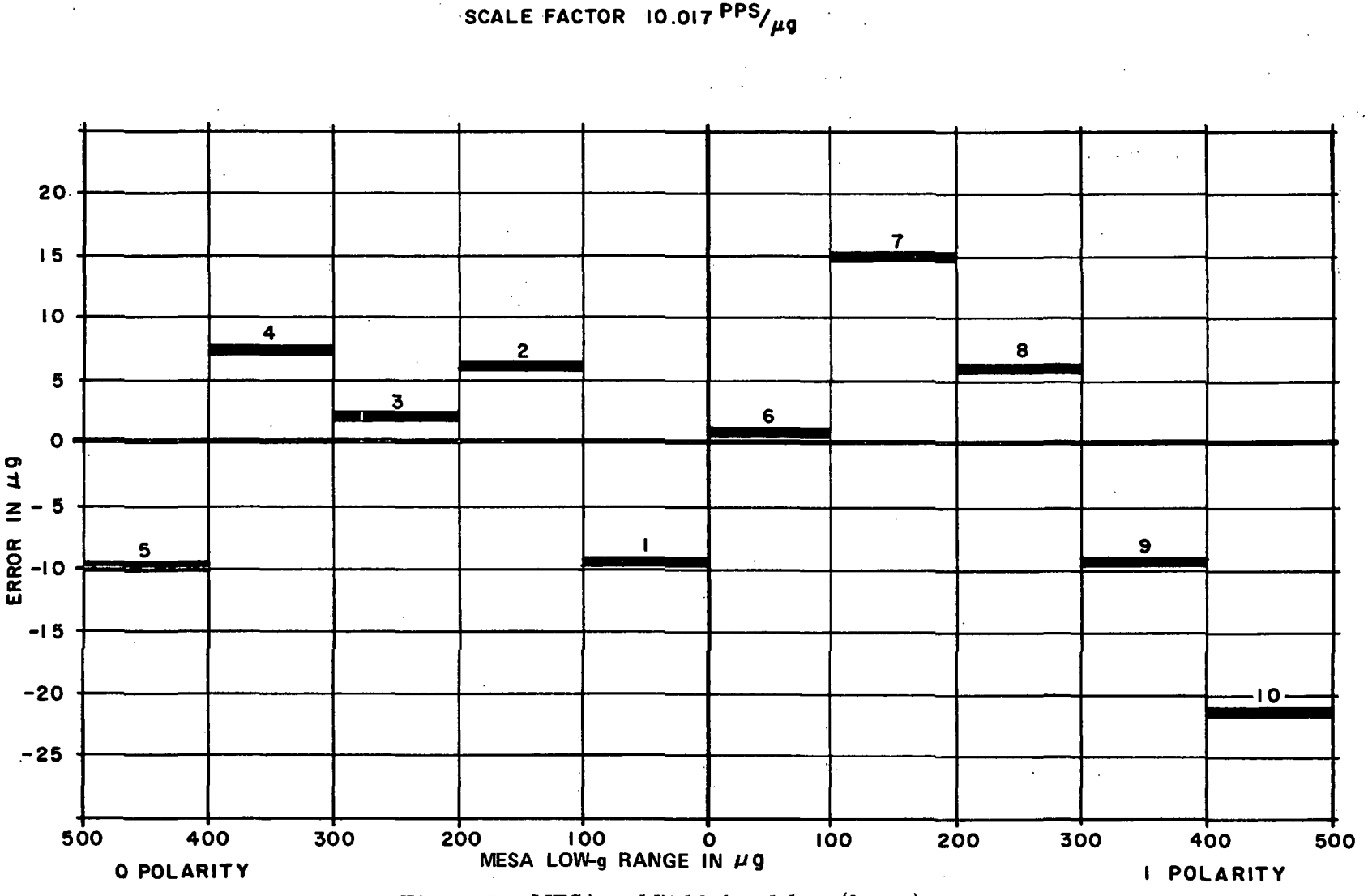

Figure 7. MESA and Wild theodolite (low g).

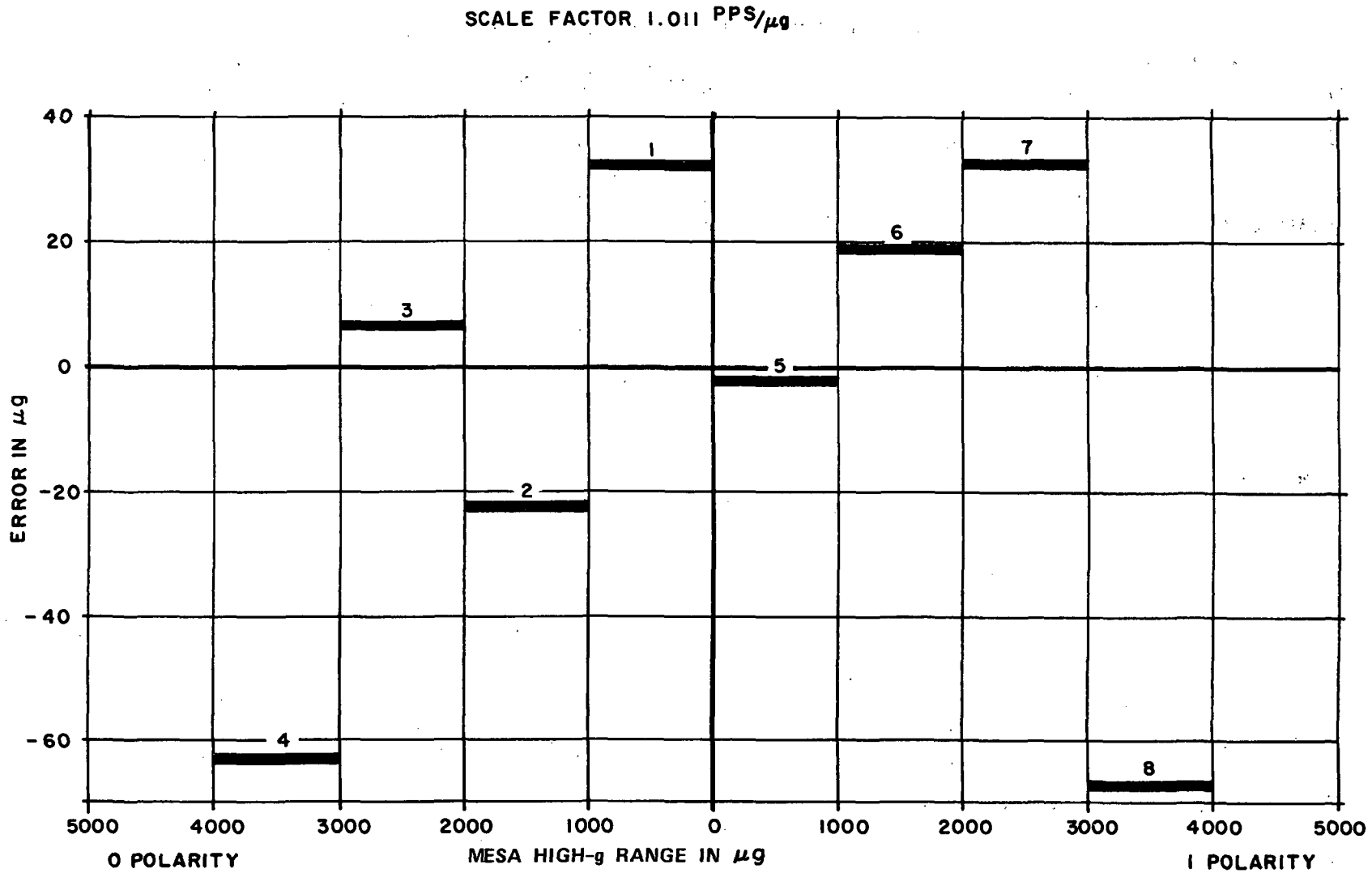

Figure 8. MESA and Wild theodolite (high g).

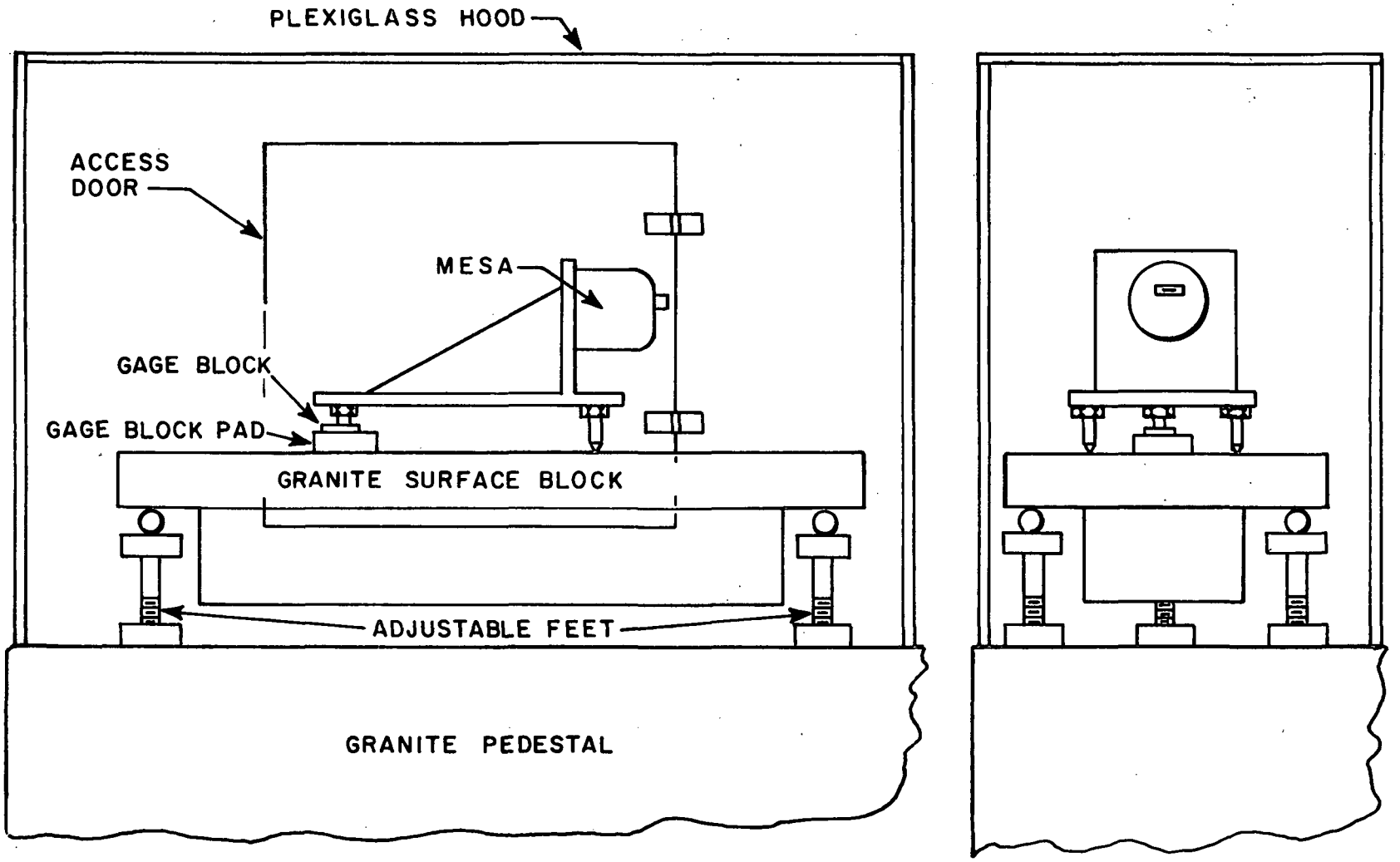

Figure 9. Gage block test arrangement.

A = 0.258 TO 0.262 cm (0.101 TO 0.103 in.)
B = 0.259 TO 0.264 cm (0.102 TO 0.104 in.)
C = 0.258 TO 0.267 cm (0.101 TO 0.105 in.)
D = 0.258 TO 0.277 cm (0.101 TO 0.109 in.)
} COMBINATION OF GAGE BLOCKS USED

MESA SCALE FACTOR 0.056 PPS/μg

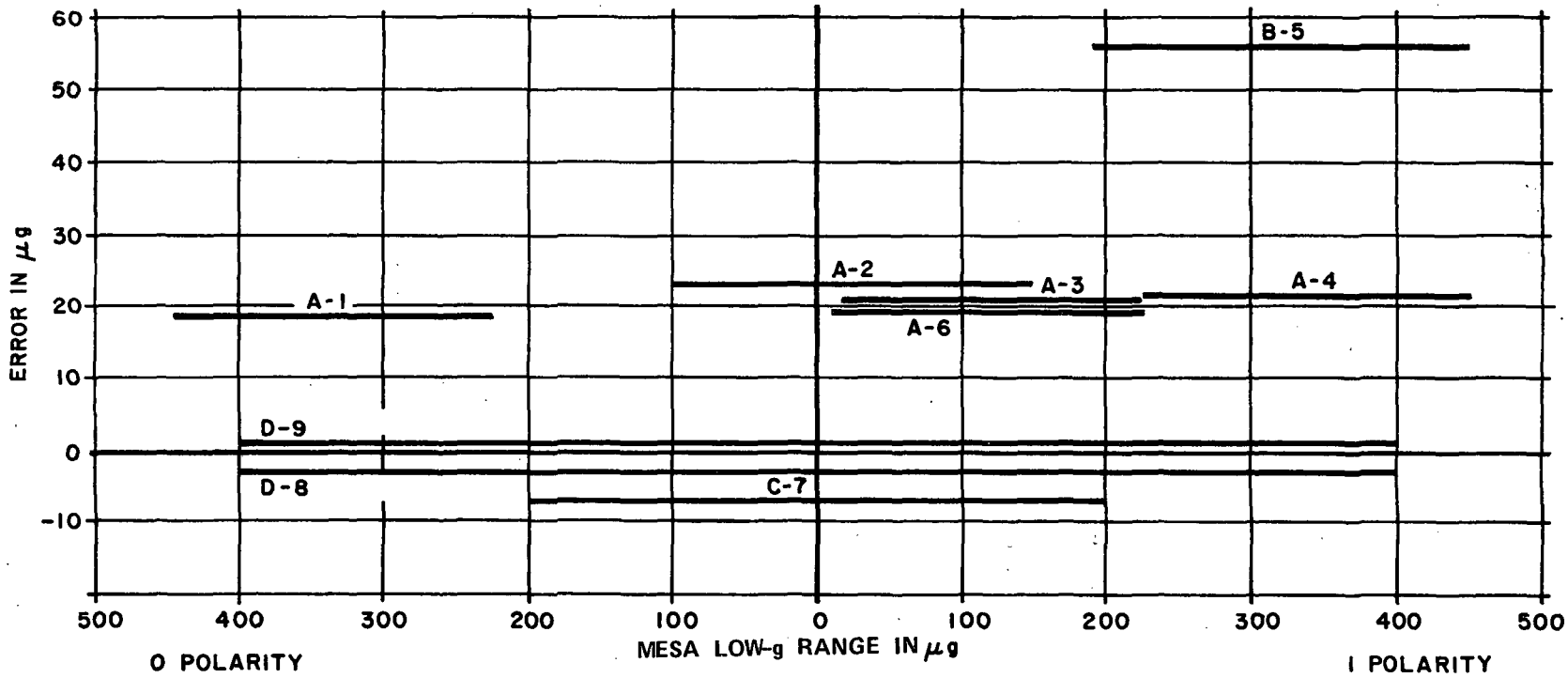

Figure 10. MESA and gage blocks (low g).

Figure 11. MESA and gage blocks (high g).

The gravitational force applied to the MESA is g sin θ. The tilt applied to the fixture is $(B_1 - B_2)/10 = \tan \theta$, where

g = earth gravity expressed as unity.

B_1 = first block.

B_2 = second block.

θ = angle between the MESA sensitive axis and the horizontal.

Since the difference between the sine, the tangent, and the angle in radians is less than 10 parts/1 000 000 for the small angles under consideration, all calculations are made in radians. The change made to the MESA is therefore $(B_1 - B_2) \times 10^5$ μg.

Figures 10 and 11 are low-g and high-g tests, respectively. The letter and number over the plots give the gage combination shown at the top of the page and the sequence in which the tests for the plot were run. It may be significant to note that the tests with each set of blocks tended to repeat without regard to the position in the MESA range, and the different sets of blocks tended to show errors characteristic to that set. The accuracies normally associated with these gage blocks are in the realm of 6.35 to 127 $\times$ 10^{-8} m (25 to 50 μin). The blocks used were not certified standards and therefore could have had much larger errors. It is also probable that some fixture temperature distortion was present since the hood had to be opened each time the blocks were changed.

Tiltmeter and Hood Cover

The following tests were made with the base of the MESA clamped in the holding fixture. Target mirrors were attached to the exposed end of the MESA base for the optical instruments used as the primary testing devices. Also, the Model DCM31 tiltmeter was mounted on the granite pedestal with the test setup so that corrections could be made to the test data when a significant seismic change in the pedestal was noted.

The MESA input was made adjustable by setting the fixture end with two bearing points on a fixed surface plate and the single bearing point end on an adjustable surface plate. Lead weights were used to adjust the weight

on the bearing points. The bearing points were positioned to provide maximum leverage or minimum movement to the MESA when adjustments were made. This allowed an adjustment sensitivity of about 3.5 μg/minor division on the adjusting screw dial as compared with 9.8 μg/minor division on the fine indicator of the dividing head when it was being used. This arrangement offered the possibility of greatly reducing the effects of heat variation errors in the fixture by virtue of measuring the displacement of the MESA directly.

Hilger Watts Autocollimator

Figure 12 shows the results of a test made with the Hilger Watts TA-51 dual axis autocollimator. In this arrangement the autocollimator was mounted on the pedestal but outside of the hood covering the MESA. A hole in the hood allowed the objective end of the autocollimator to protrude through but not touch the hood. Angular displacements were measured and converted to μg as was done with the dividing head.

The Hilger Watts autocollimator has a minor division scale of 0.2 arc-sec which is the accuracy that may be approached from many readings. The spread of the readings are normally expected to be within 1 arc-sec, which should produce a tilt angle error of less than 5 μg.

The distribution of errors in Figure 12 would suggest that the limits had been reached for (1) the autocollimator, (2) the MESA, or (3) the test setup as a whole. As with the theodolite, the results did not show the expected degree of agreement and again it may be caused by movements incurred during adjustments of the autocollimator (a test setup problem). The maximum undisturbed variations in the MESA output prior to tests were less than 0.5 μg.

Razdow Mark II Autocollimator

Figure 13 shows the results of a test with a Razdow Mark II automatic autocollimator. The Mark II is basically a precision rate measuring device; however, by proper interpretation of the output signal, it can also be used for position measurements as was done here. The output of the Mark II (monitored on a strip chart) is a voltage which varies in a near sine wave while the angle of the autocollimator to the normal of the target mirror is increased or decreased in a linear movement.

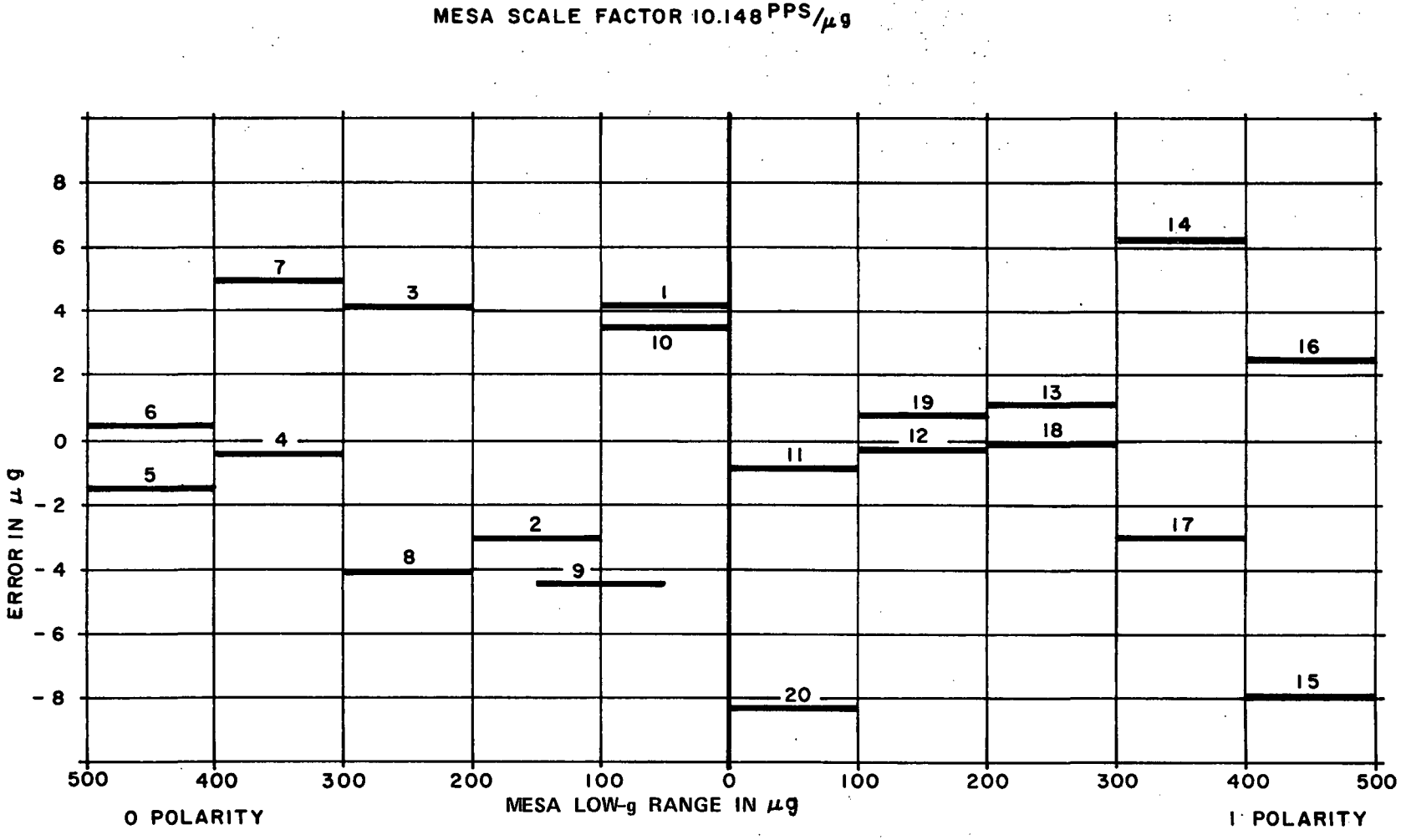

Figure 12. MESA and Hilger Watts autocollimator.

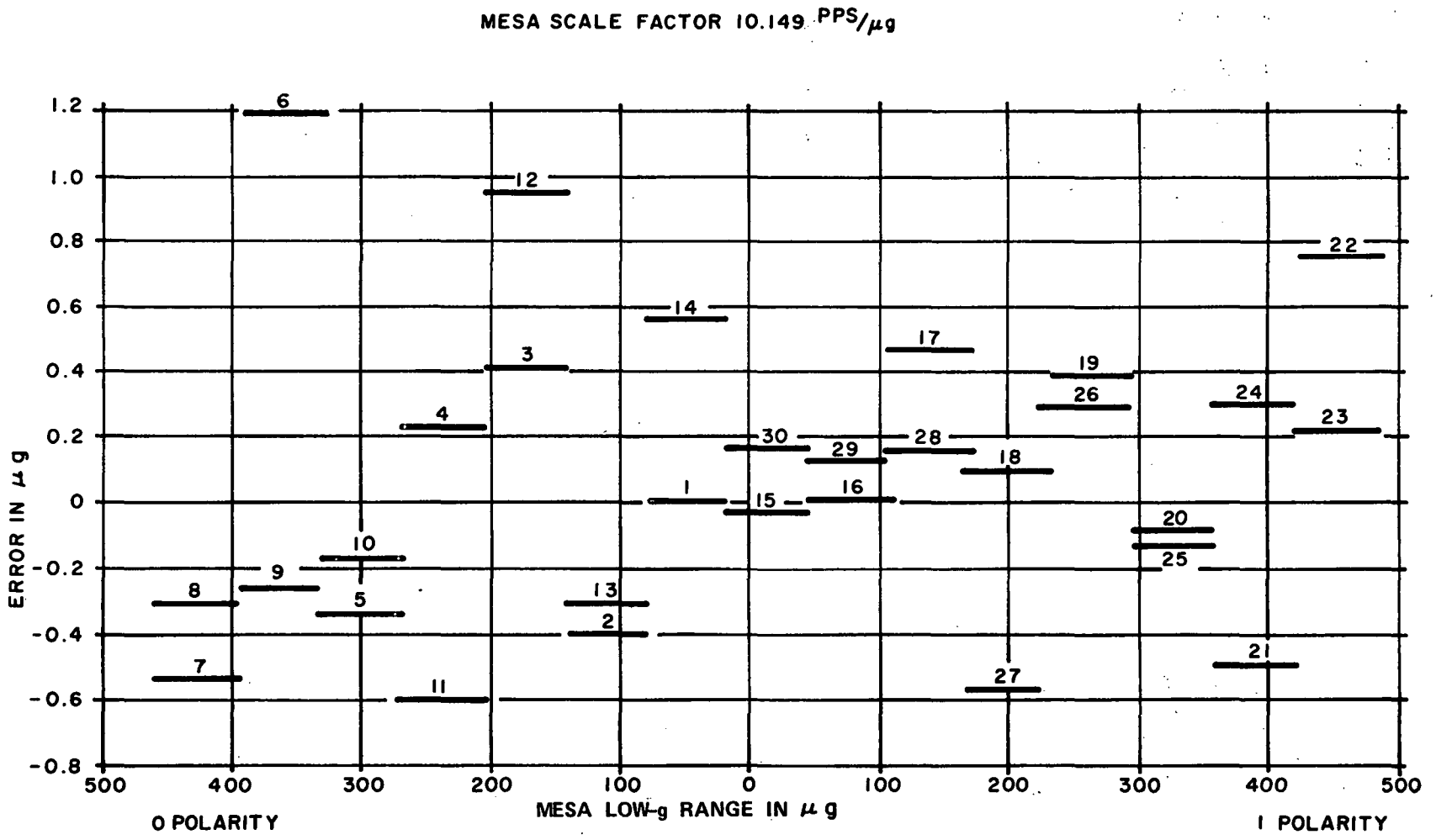

Figure 13. MESA and Razdow Mark II autocollimator.

To determine the angle between two positions which produce more than or less than an even number of cycles, the sine wave must be interpolated. This was done as given in the next paragraph.

From Figure 14, E_{max} and E_{min} are the maximum and minimum levels of the output voltage. E_1 and E_2 are the first and second readings taken at two respective positions, and N is the number of cycles in which the voltage has passed through both a maximum and a minimum level between E_1 and E_2.

$$\mu g = 0.175071 \left[360\, N \pm \sin^{-1}\left(\frac{2E_1 - E_{max} - E_{min}}{E_{max} - E_{min}} \right) \right.$$

$$\left. \pm \sin^{-1}\left(\frac{2E_2 - E_{max} - E_{min}}{E_{max} - E_{min}} \right) \right]$$

The asterisks reverse with the slope of the signal. The constant

$$0.175071 = (13 \times 4.84813)/360$$

where

4.84813 = μg/arc-sec

13 = arc-sec/cycle (scale factor)

360 = deg/cycle

μg = change in μg to which the MESA is subjected when the Mark II output voltage changes from E_1 to E_2.

A typical example of a measurement with the Mark II is as follows, where

E_1 = 59 V

$E_{max\ 1}$ = 110 V (first max following E_1)

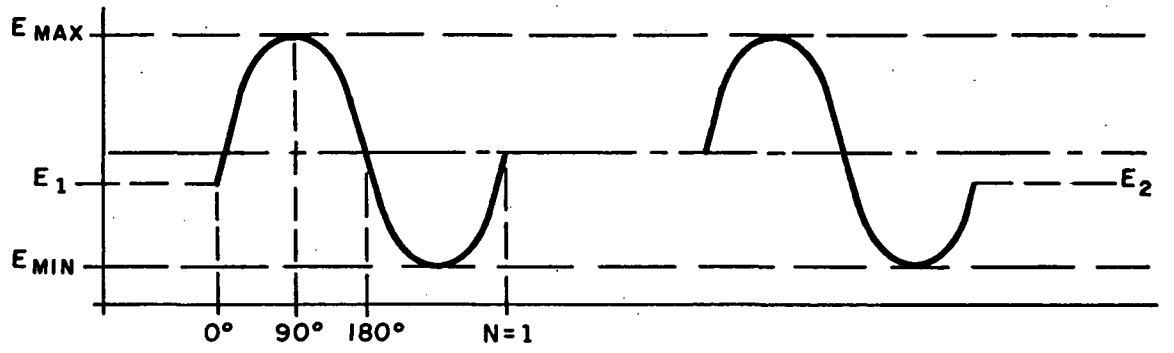

Figure 14. Razdow output.

$E_{min\ 1}$ = 10 V (first min following E_1)

N = 2

E_2 = 60 V

$E_{max\ 2}$ = 113 V (last max preceding E_2)

$E_{min\ 2}$ = 13 V (last min preceding E_2),

$$\mu g = 0.17507\left[360 \times 2 + \sin^{-1}\left(\frac{2 \times 59 - 110 - 10}{110 - 10}\right) + \sin^{-1}\left(\frac{2 \times 60 - 113 - 13}{113 - 13}\right)\right] = 0.17507\left[720 + \sin^{-1}(-0.020) + \sin^{-1}(-0.040)\right] .$$

Since the equation is set up for angular degrees, the first inverse sine term is equal to 1.1 deg and the second is equal to -2.3 deg. The total displacement is equal to 0.17507 (718.8) μg or 125.83 μg.

A series of readings were taken through the range of the MESA so that, for each successive plot, E_2 of the previous sample becomes E_1 of the next. All values of E_1 and E_2 were taken as near as possible to the sine 0 and sine 180-deg level to obtain maximum accuracy from the Mark II.

The manufacturer had calibrated the Mark II by comparing it with another autocollimator. Ten successive samples of about 3240 arc-sec each were averaged to derive a scale factor of 13 ± 0.02 arc-sec/cycle.

In the tests with the MESA, errors of less than ± 1 μg (± 0.2 arc-sec) could be maintained by careful selection of the test points. Figure 13 shows a typical test with the Mark II where the output voltage angle is kept small. Of this error, ± 0.2 μg could be attributed to the MESA output variation.

Of the electronic systems, the Razdow Mark II was the less difficult to align, the least temperature sensitive, and provided the greatest range. However, the output of the Razdow was inclined to drift, was nonlinear and therefore difficult to interpolate, and subject to a variable error which at the maximum made the system little more precise than the manual autocollimator. The Razdow therefore would not be the best choice to make measurements of an independent input which may fall into its areas of low accuracy.

One of the main sources of error in the Mark II appears to be in the variation or drift of the output voltage levels. This was large enough to cause a calculated error of about 1 μg at the zero angular level and about 4.5 μg at the 90-deg level (Fig. 14). This error would not likely be significant in the calibration method used for the Mark II but does become significant for the small angles used in these tests.

Laser Interferometer Measuring System

Figure 15 shows the test setup using the General Dynamics laser interferometer measuring system as the primary testing system and the Ideal Aerosmith DCTM31 tiltmeter as the test stand level. For clarity, the laser tube, photomultiplier, tiltmeter electronics, and MESA electronics are not shown in Figure 15. All lead wires and cables leading off the pedestal shown discontinued were taped or tied to the pedestal so that a minimum of vibration or movement would be transferred to the equipment on the pedestal.

The interferometer system is normally used to measure precision parts on gyros and accelerometers. For this, it is used on a spring-cushioned optical bench. Portable unit heads shown in Figure 16 (a) were provided for making other measurements where it is not possible to work on the bench. Fiber optics are provided to connect the laser source and other electronics to the unit heads. (A visual alignment system that is normally used on the bench cannot be used in this arrangement.)

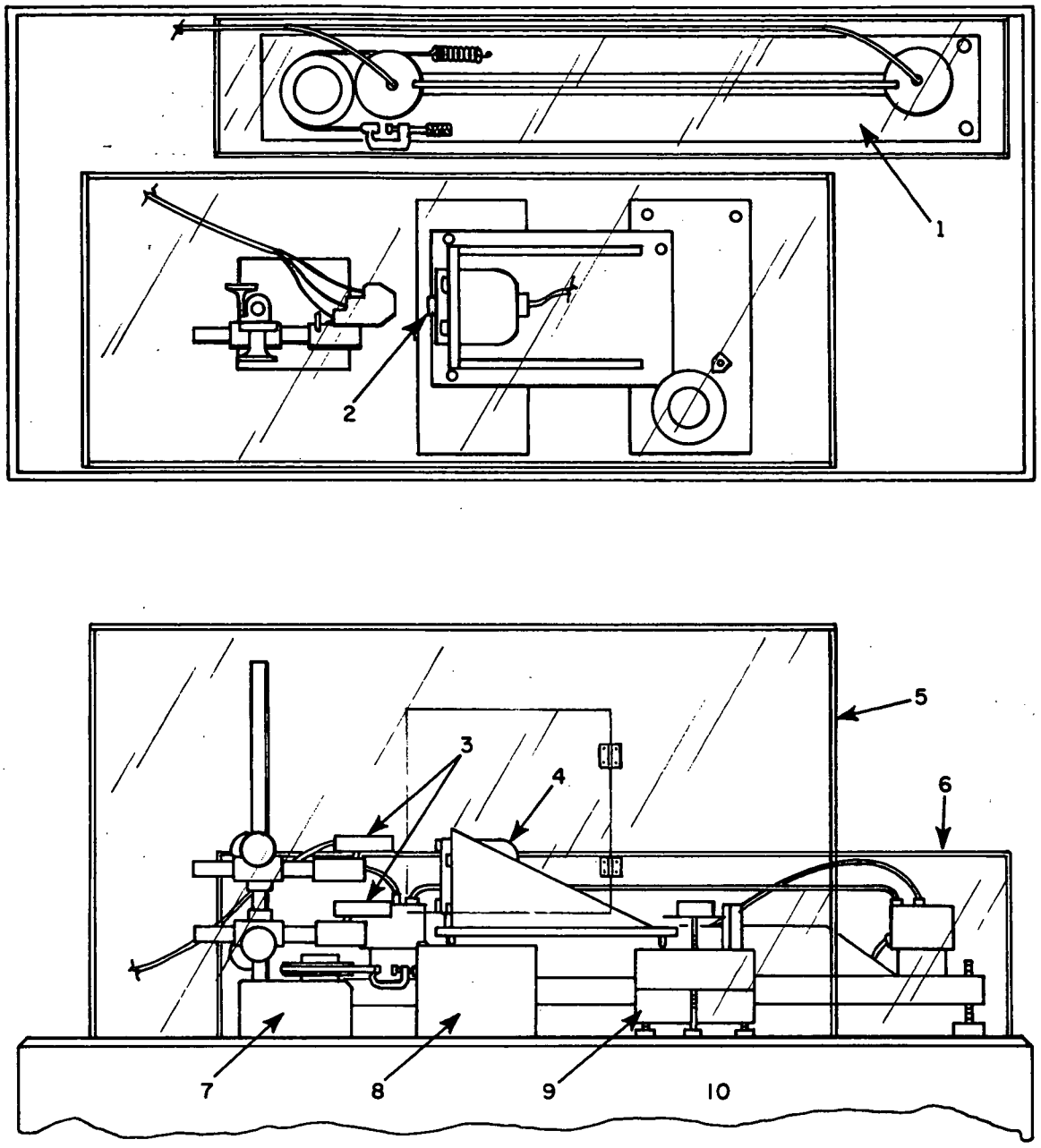

1 - TILTMETER
2 - MIRRORS
3 - INTERFEROMETER MEASURING HEADS
4 - BELL MESA
5&6 HOODS
7 - GAGE STAND
8 - FIXED SURFACE PLATE
9 - ADJUSTABLE SURFACE PLATE
10 - GRANITE PEDESTAL

Figure 15. Interferometer system test setup.

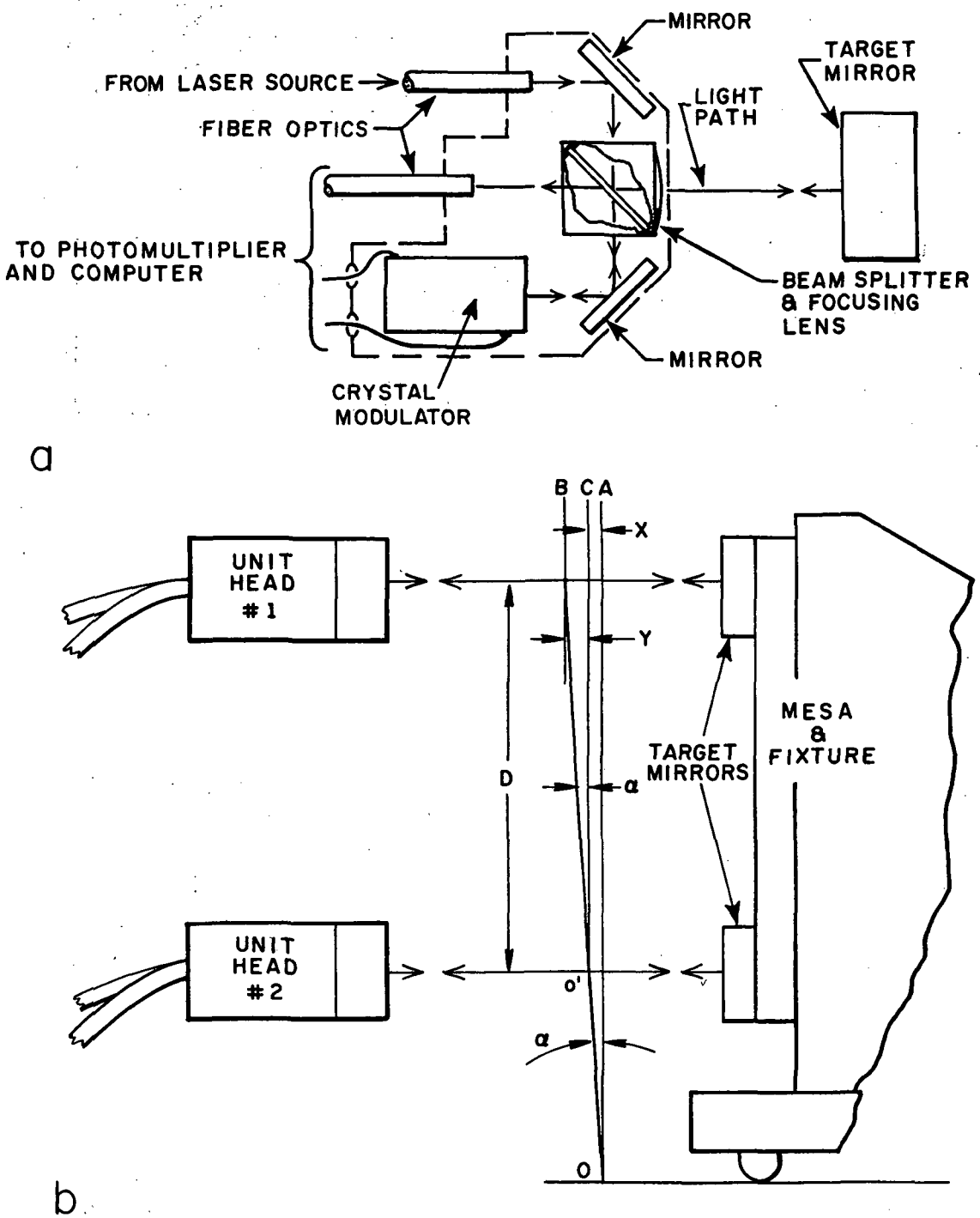

Figure 16. Unit interferometer measuring head and measurement geometry.

The output display consists of a digital readout and an analog voltage with meter readout. The digital readout provides a count of the number of half wavelengths that a target mirror may be moved away from or toward the unit head. The analog voltage is a ramp which provides the fractional part of the last (units) digit. In the mode used for the MESA test, a difference count was used; i. e., the unit head No. 2 distance was subtracted from unit head No. 1 distance and displayed.

The measurements were made as shown in Figure 16 (b). If the reference line AO is parallel to the mirror surfaces at the initial position and BO is parallel after the fixture and MESA have been moved through an angle (the size of α is exaggerated on the drawing for clarity), the distance Y will be indicated on the display. The distance X will have been subtracted from the display because the readout shows only the difference in movement of the target mirrors. The change in input to the MESA is proportional to the ratio of KY/D where Y is the display reading, D is the spacing between the light beams, and K is a dimensional constant.

A typical example of a measurement with the interferometer system is as follows:

1. With the mirrors parallel to AO, the display reads +100 and the analog meter reads 55.

2. The MESA is tilted so that the mirrors are parallel to BO. The display now reads +95 and the analog meter reads 50.

3. The spacing between the beams is 10.300 cm (4.050 in.).

4. A half wavelength of the laser light is 31.60×10^{-8} m (12.45 μin.) (one digital count).

5. The change in input to the MESA is 15.52 μrad (1 μrad of tilt produces 1 μg of input).

The laser interferometer system as shown offered the possibility for the greatest accuracy of any of the measuring arrangements shown. The wavelength of the laser light is known to within 0.5 percent. This would then be the upper limit of accuracy available.

The target mirrors were accurate to 0.75 wavelength. This would allow a maximum error of about 10.16×10^{-8} m (4 μin.) which would cause

an error of about 1 μg. However, this error is reduced if the point where the beams impinge on the target mirrors could be made to stay in nearly the same spots.

Another error caused from lateral movement develops from the light beams and mirrors not being exactly parallel. For the example shown, an error of 0.07 μg would result from each 0.254 cm (0.001 in.) of lateral movement in the fixture for 1 min of error in the mirror alignment. Mirror alignments were somewhat difficult to obtain but could be accomplished with special care; however, the lateral movement may be extremely difficult to overcome.

These errors probably account for most of the randomness of the adjacent plots where the test is progressing in one direction through the MESA range. Because the readings were taken sequentially, a reading error that causes one plot to be low will cause the next to be high on the error scale. This is typical in Figure 17 where the measuring system was set to zero with the accelerometer at zero for the measurements in each direction.

Temperature changes in the test stands holding the interferometer units probably contributed the main error (probably 2 or 3 percent) to the overall scale factor.

Like the Razdow, the laser interferometer system readout was subject to cyclic error. In the laser system this error was present when the ramp voltage of the analog readout approached the crossover at the ends of the ramp. Because of the higher seismic vibrations and the high repetition rate of the readout system, the average output was obscured between the upper and lower ends of the ramp as the unit's digits hovered between two numbers. Under these circumstances, the analog meter would read the average between the high and low samples. This caused the meter to give an erratic reading. In the course of testing, the only way to avoid this problem was to adjust the MESA position so that all readings fell well within the ramp area of the analog readout.

Figure 18 shows the effects of two of the problems mentioned. The loop effects on the right side is typical of that caused by a continuous temperature change. The sloping change on the left side is typical of mirror misalignment with the lateral movement of the fixture. In this case the movement is somewhat linear but this was not always so.

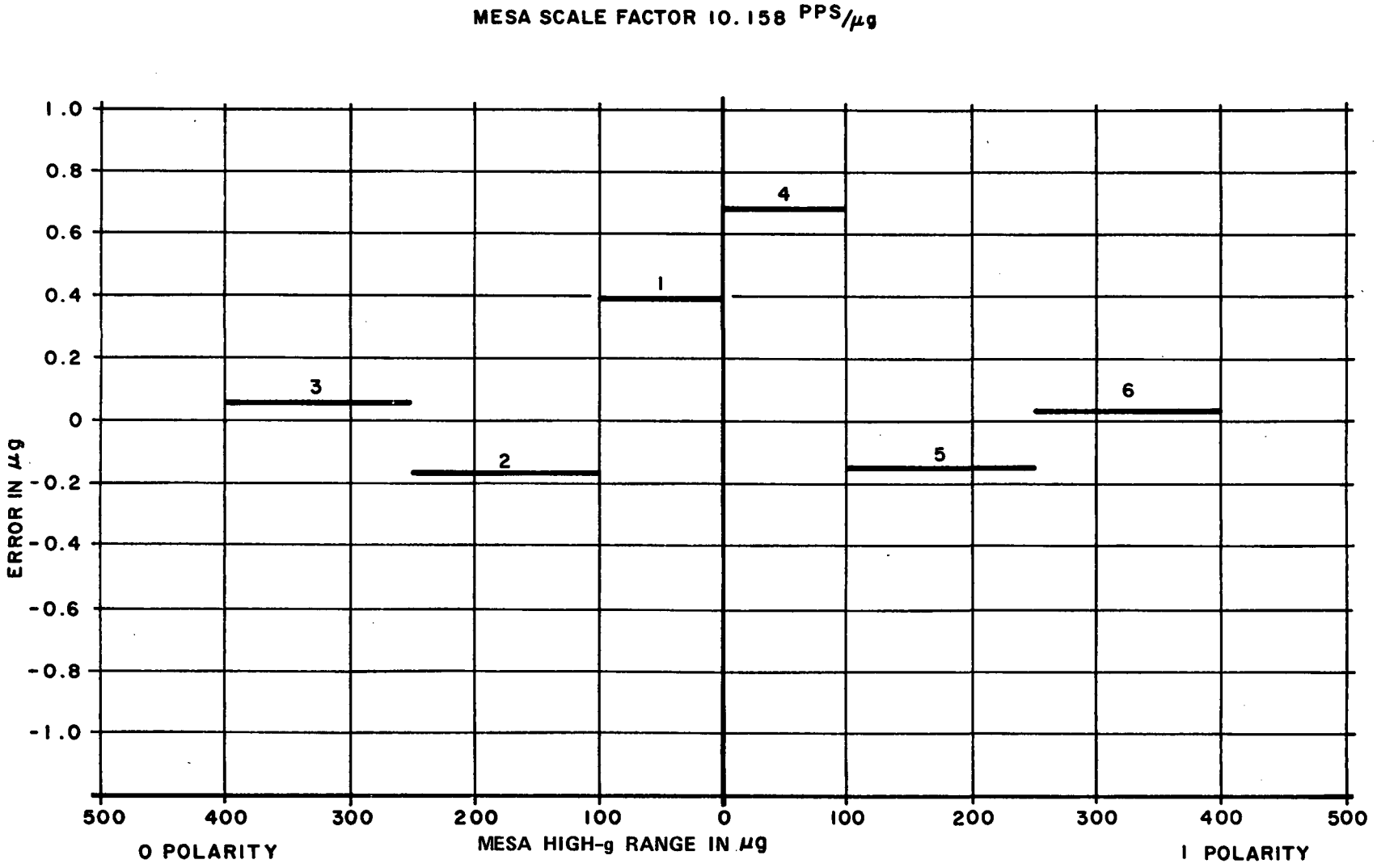

Figure 17. MESA and Interferometer System Test No. 1.

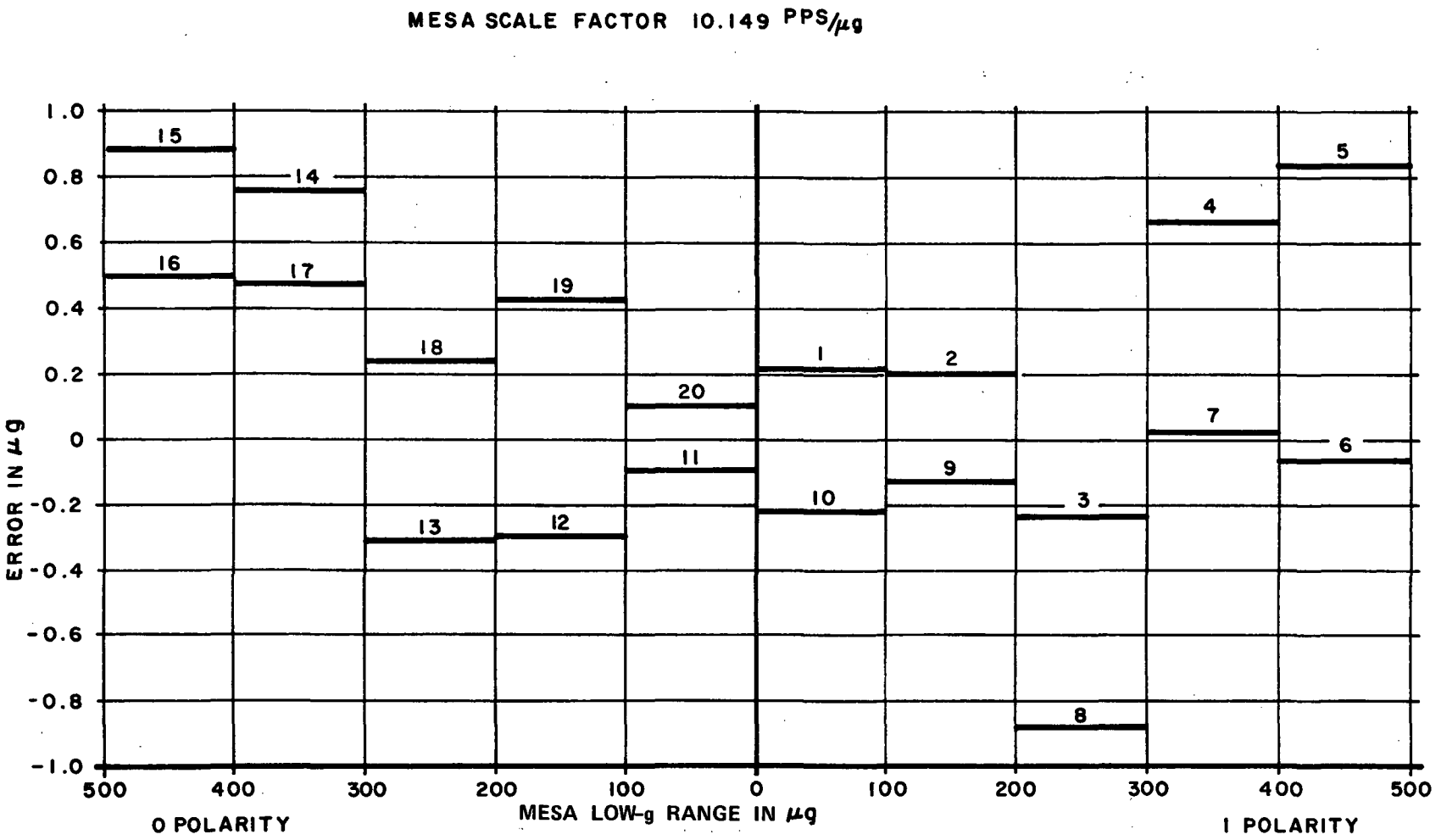

Figure 18. MESA and Interferometer System Test No. 2.

Figure 19 is a test in which a number of passes were made over the same area of the MESA range. These variations are probably caused by uneven lateral movement errors along with mirror surface irregularities and mirror misalignment.

Because of wear and slippage in the screw bearing surfaces on the adjustable surface plate, the lateral position of the fixture was caused to change. Because of this, the fixture may be moved and returned to the same vertical position but may not necessarily come back to the same lateral position. The lateral movement was sometimes quite consistent as in Figure 18 and at other times random as in Figure 19. This problem could be observed when the setup was used in the tests with the Hilger Watts dual axis autocollimator. Although only a lateral angular displacement could be observed in these tests, it can be assumed that lateral displacement was encountered because of the fixture bearing point arrangement.

Figure 20 is a repeat of Figure 17 but with the measurement made through the MESA range and back to the starting point.

The test setup using the laser interferometer system was potentially the most accurate test method available. It was also the most difficult to set up and operate. The gage stand used to mount the unit heads was not very satisfactory because the adjustments were too crude for the rather fine adjustments which the interferometer heads require. Also drift tests indicated that the stand and the unit head were probably affected by the higher frequency vibration and temperature change mentioned earlier. If this method were to be used regularly, it is recommended that a well designed fixture with very precise adjustments for the unit heads be made or the optical table be adapted to the test pedestal.

OTHER TESTS OF MESA

Acceptance Tests

The acceptance tests were run on the Leitz dividing head without benefit of the tiltmeter or hood. The acceptance test procedure for the MESA system which was supplied by the manufacturer was run without problems except in the tests for output stability. These tests were found to fail as frequently as not. Later investigations into the seismic and temperature problems confirmed that the inputs to the MESA had not been properly maintained. Later data gave evidence that the unit was well within these specifications.

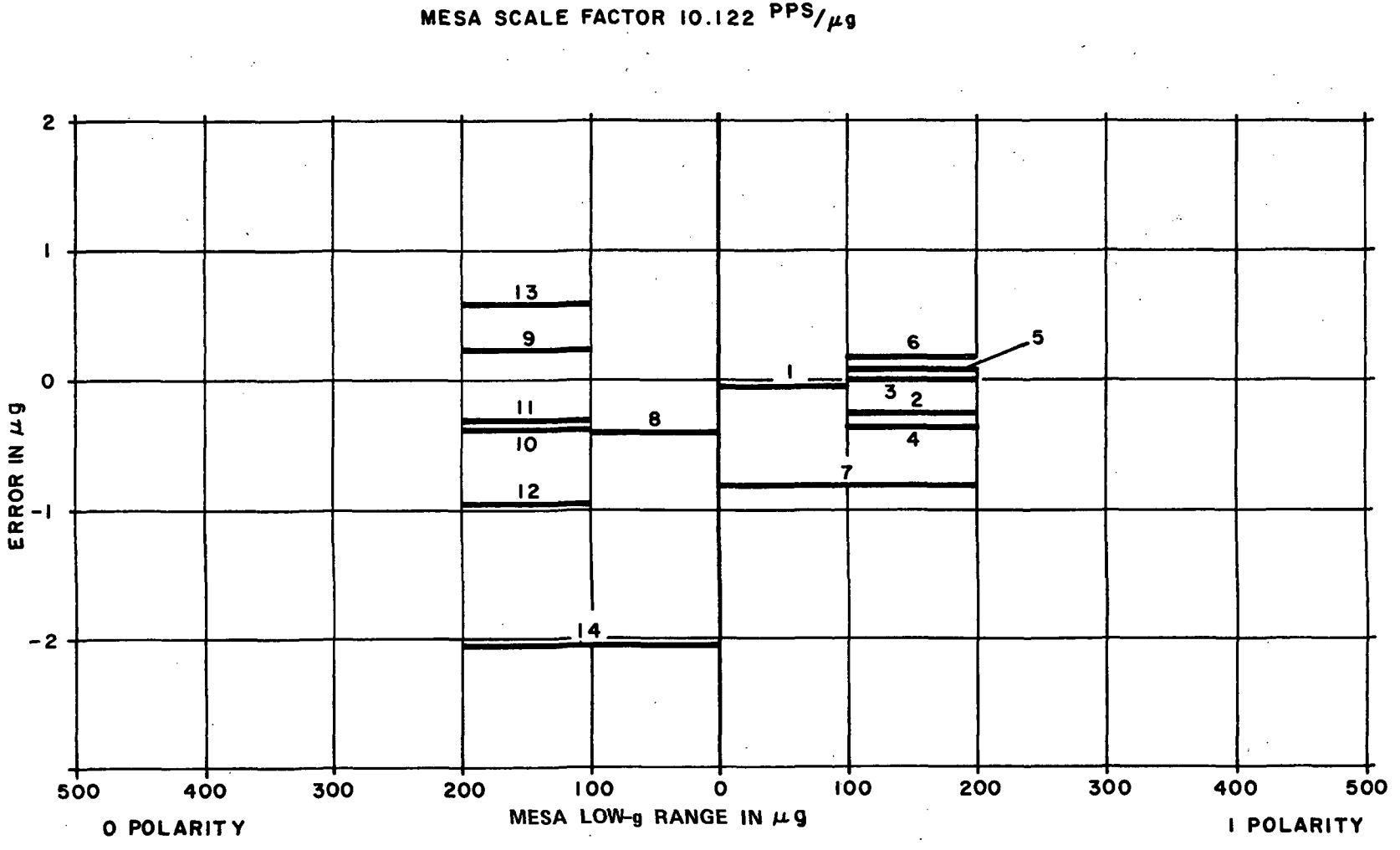

Figure 19. MESA and Interferometer System Test No. 3.

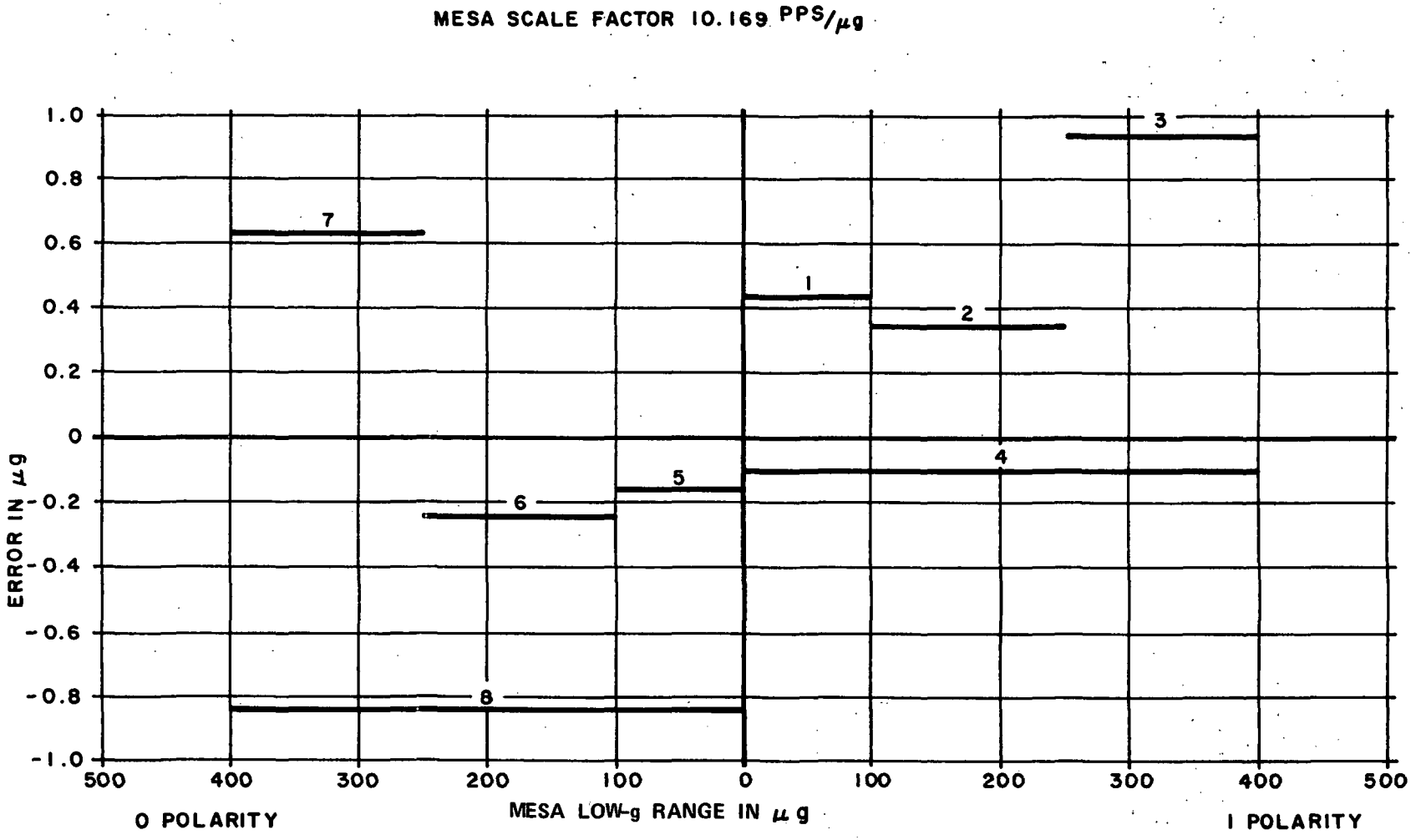

Figure 20. MESA and Interferometer System Test No. 4.

Temperature Vs Scale Factor Tests

Using the Razdow autocollimator because it was less vulnerable to temperature changes, some tests were made to observe the effects of temperature changes in the MESA scale factor. Heaters were attached to the fixture and the MESA so that a small amount of extra heat could be applied (but not enough to override the oven). Three tests were run at elevated temperatures alternately with three tests at normal temperature. Adequate stabilization time was allowed for each. The change in scale factor averaged about 0.1 percent increase for each degree centigrade increase when calculated over 80 percent of the MESA range.

Crossover Point

The limitations imposed by environmental conditions prevented a close examination of the crossover point. However, in tests where the test sample was taken through the crossover point as in Figure 13, no change in output error was apparent. A discontinuity was observed which had a "ball in a box" characteristic when a changing input caused the MESA to pass through the zero point, but the response was normal after crossover.

Running Time

The operating time on the MESA under test at the time of this writing is about 29 000 hr with no apparent degradation of performance. The running time between the first calibration test in Figure 5 and that in Figure 20 was caused by the more precise test methods and improved environmental conditions.

CONCLUSIONS

MESA Linearity

The output of the MESA was as linear and consistent as any of the available devices were capable of measuring. Although the extent of agreement varied with the test equipment used, it can only be concluded that the indicated errors were attributable to the test equipment coupled with the environmental conditions. In some cases the errors were larger than the expected or published errors for the equipment involved; yet the MESA agreed with the most precise methods and the expected limits of the test equipment.

Equipment Variation

Figure 21 is a comparison of the various test systems. The RMS error was calculated from the error increments of the indicated test plots. The MESA contribution was calculated from samples of the test run while no input changes were being made. This is the RMS magnitude of variations of the MESA output with fixed input for the tests involved. This contribution was larger, as shown, in the tests with the dividing head and the theodolite because the hood was not being used and the fixtures and test equipment were being exposed to normal room environment.

Equipment Comparison

Figure 21 shows that the automatic readout systems were subject to much less error than the manual equipment. This is reasonably so because automatic systems were set up under the hood and could remain undisturbed during the tests.

Of the automatic equipment, the laser interferometer system offered the nearest to a primary standard of measurement because the unit of measurement is known very precisely and it is very constant. However, the Razdow Mark II offered a more expedient means of making the tests but the calibration methods used were of questionable value for this purpose. With the suggested improvements discussed previously, the interferometer system offers the most precise method of testing small angles as used on low-g accelerometer testing.

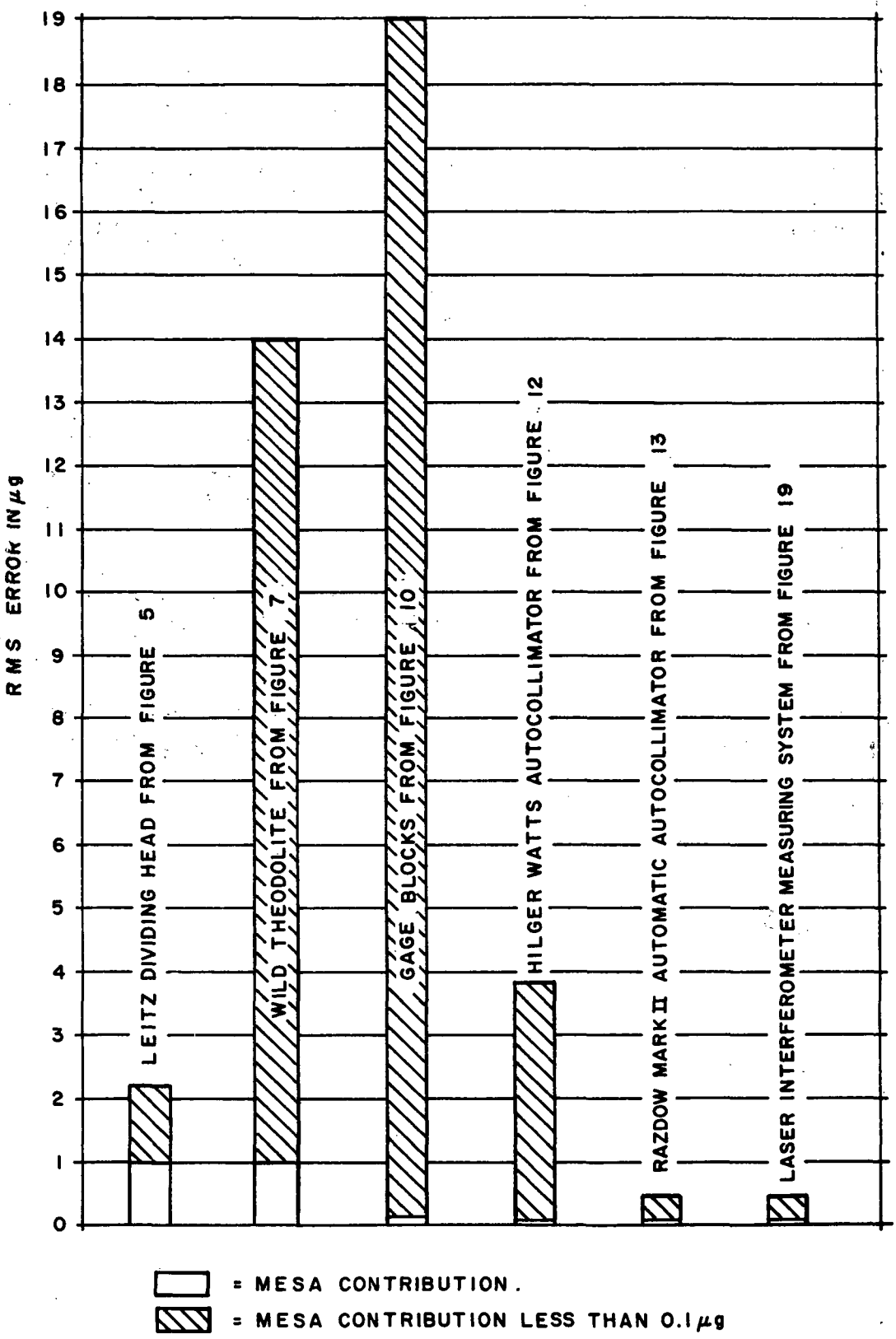

Figure 21. RMS error comparison.

REFERENCES

1. Lesco, Daniel J.: Flight Evaluation of an Electrostatic Accelerometer for Measurement of Low-Level Orbital Accelerations. Lewis Research Center, Cleveland, Ohio.

2. Reinel, Konrad: Accelerometer Calibration in the Low-g Range by Means of Mass Attraction. NASA TM X-53837, Marshall Space Flight Center, Alabama, June 27, 1969.

APPROVAL

LOW-g ACCELEROMETER TESTING

By Bobby F. Walls and Miller S. Vaughan

The information in this report has been reviewed for security classification. Review of any information concerning Department of Defense or Atomic Energy Commission programs has been made by the MSFC Security Classification Officer. This report, in its entirety, has been determined to be unclassified.

This document has also been reviewed and approved for technical accuracy.

P. H. Broussard Jr

P. H. BROUSSARD, JR.
Sensors Branch

C. H. Mandel

C. H. MANDEL
Guidance and Control Division

F. B. Moore

F. B. MOORE
Director, Astrionics Laboratory

MSFC—RSA, Ala

Page Intentionally Left Blank

DISTRIBUTION

INTERNAL

DIR
DEP-T
AD-S
A&TS-MS-H
A&TS-MS-IL (8)
A&TS-MS-IP (2)

PD-AP-DIR
Mr. Stewart

PD-DO-DIR
Dr. Thomason

PM-SL (AAP)
Mr. Ise (3)

PM-PR-M

S&E-DIR
Mr. Richard

S&E-CSE-DIR
Dr. Haeussermann

S&E-CSE-A
Mr. Hagood
Mr. Hunter

S&E-P-ATM
Mr. Cagle

S&E-ASTR-DIR
Mr. Moore
Mr. Horton

S&E-ASTR-A
Mr. Hosenthien
Miss Flowers

S&E-ASTR-B
Mr. Kampmeier
Mr. Rowell
Mr. Spears
Mr. Ham

S&E-ASTR-C
Mr. Swearingen

S&E-ASTR-E
Mr. Aden

S&E-ASTR-G
Mr. Mandel
Dr. Doane
Mr. Wood
Mr. Jones
Mr. Doran
Mr. Broussard
Mr. Morgan
Mr. Kelley
Mr. Lee
Mr. Kalange
Mr. Smith
Mr. Fikes
Mr. Gaines
Mr. Walls (25)

S&E-ASTR-I
Mr. Duggan

S&E-ASTR-M
Mr. Boehm
Mr. Allen

S&E-ASTR-R
Mr. Taylor

S&E-ASTR-S
Mr. Wojtalik
Mr. Noel
Mr. Brooks

A&TS-PAT
Mr. Wofford

A&TS-TU (6)
Mr. Winslow

S&E-ASTR-ZX

EXTERNAL

Scientific and Technical Information
Facility (25)
P. O. Box 33
College Park, Maryland 20740
Attn: NASA Representative
(S-AK/RKT)

National Aeronautics and Space
Administration
Washington, D.C. 20546
Attn: Mr. Theodore Michaels, REG
Dr. Peter Kurzhals, REG (5)
Mr. Carl Janow, REG
Mr. Authur Reetz, Jr., RX
Mr. Richard Livingston, MTG
Mr. William Hamby, HLO

Langley Research Center
National Aeronautics and Space
Administration
Langley Station
Hampton, Virginia 23365
Attn: Mr. Keckler (5)

Bell Aerospace Company
P. O. Box 1
Buffalo, New York 14240
Attn: Mr. Bill Lang (5)

Sperry Space Support Division
Dept. 561
716 Arcadia Circle, N. W.
Huntsville, Alabama 35801
Attn: Mr. Miller Vaughn (5)
Mr. Dan LeBas (5)

Department of the Air Force
Air Force Avionics Laboratory
Wright Patterson A. F. B., Ohio 45433
Attn: Mr. Bob McAdory (5)
AFAL-NVN

U. S. Army Missile Command
Research and Development Directorate
Redstone Arsenal, Alabama 35812
Attn: Mr. J. V. Johnston (5)
Mr. Joe Hunter (2)